

## RADIOGENIC ARGON RELEASED BY STEPWISE HEATING OF GLAUCONITE AND ILLITE: THE INFLUENCE OF COMPOSITION AND PARTICLE SIZE

A. A. HASSANIPAK<sup>1</sup> AND J. M. WAMPLER<sup>2</sup>

<sup>1</sup> Department of Mining Engineering, Faculty of Engineering, Tehran University, Tehran, Iran

<sup>2</sup> School of Earth and Atmospheric Sciences, Georgia Institute of Technology, Atlanta, Georgia 30332-0340

**Abstract**—Various size fractions of several samples of glauconitic clay and illite were heated stepwise under vacuum for extended periods to: 1) evaluate radiogenic-argon (Ar) yields in relation to composition and size range; and 2) investigate the kinetics of radiogenic-Ar release. Each sample was heated at 250, 375, 500 and 1000 °C.

The radiogenic-Ar release patterns are nearly the same for the various size fractions of each sample. The Ar yields are not functions of particle size, at least not in these size ranges. This observation suggests that the kinetics of radiogenic-Ar release from these materials under these experimental conditions may be controlled by some mechanism other than diffusion.

The experiments show distinct differences in yield of radiogenic Ar from glauconitic clay and illite, which were most evident in the 375 and 500 °C steps. The yield (relative to the total amount of radiogenic Ar in the sample) at a particular temperature is inversely related to potassium (K) content, and there appears to be a direct dependence of yield on the iron (Fe) content. Because the literature provides evidence that Ar release during heating of phyllosilicates under vacuum is controlled by dehydroxylation and also provides evidence that dehydroxylation of clay may follow first-order kinetics, the kinetic data on Ar release from these samples were compared to simulated first-order reactions. To match the observational data requires more than 2 activation energies in each simulation, which is consistent with the known mineralogical heterogeneity of such samples.

**Key Words**—Argon, Dehydroxylation, Glauconite, Illite.

### INTRODUCTION

For more than 3 decades there has been continual interest in the influence of particle size on the K-Ar ages of clays, starting with the work of Hurley and his coworkers (Hurley 1966), and in the kinetics of the release of Ar from clay, in particular glauconitic clay, during heating. There was an early concern that very fine clay particles would not retain Ar well in natural environments having only slightly elevated temperatures (Evernden et al. 1960), but later work has allayed this concern (Zimmermann and Odin 1977). The effect of increasing temperature on the K-Ar ages of fine particles in sediments has proved to be primarily a matter of diagenetic change rather than of Ar diffusion (Weaver and Wampler 1970; Aronson and Hower 1976; Liewig et al. 1987).

The association of Ar loss with H<sub>2</sub>O loss during laboratory heating of mica-like minerals, including glauconite and illite, was established long ago (Evernden et al. 1960; Polevaya et al. 1961; Sardarov 1961, 1963). Evernden et al. (1960) showed that Ar loss occurs much more readily during heating under vacuum than during heating under hydrothermal conditions. The more rapid Ar loss under vacuum was attributed to the structural disruption caused by H<sub>2</sub>O loss. More recently, studies of the dehydroxylation of micas and clays have provided insight on how particle size influences hydroxyl H<sub>2</sub>O loss (Stoch 1984, 1991).

There is renewed interest in the factors that influence the release of Ar from clays during heating under vacuum, because techniques have been developed to minimize the problem of <sup>39</sup>Ar recoil in <sup>40</sup>Ar/<sup>39</sup>Ar studies of clay samples (Smith et al. 1993; Dong et al. 1995). Among the questions that need further investigation are: 1) How does the yield of radiogenic Ar, as a function of temperature and heating time, depend upon the particle size of illitic and glauconitic clays?; and 2) How does the yield of radiogenic Ar, and thus the activation energy for the process by which Ar is released under vacuum, depend upon the chemical composition of the clay minerals?

The experiments reported in this paper were intended to provide evidence toward answering these questions, in the hope of finding a basis for better understanding the mechanism by which Ar is released from clays during heating under vacuum. Such understanding should aid in the interpretation of K-Ar apparent ages for such materials, particularly when stepwise heating is used in <sup>40</sup>Ar/<sup>39</sup>Ar studies.

### SAMPLE DESCRIPTIONS AND ANALYTICAL PROCEDURES

Four glauconitic clay samples and 2 illite samples were used in this study. A brief description of each sample is given in Table 1. For each of the samples except the Bashi pellets, 2, 3 or 4 size fractions were prepared

Table 1. Sample descriptions.

Sample name	Description
EI	Illite from shale parting in the Mississippian Madison limestone (sample location unknown)
HI	Illite from hydrothermal breccia in the Pennsylvanian Sandia Formation, Valles Caldera, New Mexico
G294†	Glauconitic pellets, Ordovician; Basal Arenigian Stage, Stora brottet, Latorp, Sweden
G1392†	Glauconitic pellets, Jurassic: Lower Oxfordian Stage, core from well near Weilheim, Germany
TWG	Highly glauconitic sand interbedded with the Eocene Twiggs Clay, Houston County, Georgia. A subsample called "TWG pellets" consisted of larger glauconitic pellets hand-picked from the original material.
Bashi	Glauconitic pellets from the Lower Eocene Bashi Marl Member, Clay County, Georgia

† Portions of samples used by Thompson and Hower (1973, 1975), who indicated that the samples had been provided to them by J. Obradovich. G294 corresponds to sample KA 294 of Evernden et al. (1961).

by settling in a centrifuge. Because of the potential importance of particle size for Ar release, the diameters of 300 particles from 1 size fraction (TWG 2–0.5  $\mu\text{m}$ ) were measured by transmission electron microscopy. The resulting size distribution is gently peaked between 1.2 and 1.6  $\mu\text{m}$ , and only about 20% of the particles have diameters outside the nominal range.

The preparation of the clay samples for Ar and K analysis was based upon a technique described by Wampler et al. (1985), which allows the sample used for Ar analysis to be recovered for the K analysis as well. Clay samples were placed in capsules prepared from fused-quartz tubing. The capsules, having an inside diameter of 2 or 3 mm and a length of 5 cm, were etched in hydrofluoric acid to remove any superficial K and then preheated in vacuum to reduce atmospheric Ar before use. After a sample had been placed inside a capsule, at its closed end, a portion of the capsule near the open end was heated to softening with a narrow flame and drawn out to form a capillary about 10 cm long. This heating and drawing were done quickly, and the capsule was cooled in  $\text{H}_2\text{O}$  immediately afterward, so little heat was transferred to the portion of the tube containing the clay. Such a capillary is long enough so that most of it remains cool as a sample is heated under vacuum to study Ar release, so any K-bearing substance that might evaporate from the clay at 1000 °C should condense in the capillary. After Ar analyses had been completed, the capsules were removed from the Ar-extraction line so that their contents could be analyzed for K and Fe.

Before the stepwise heating of individual samples was begun, the samples in a group, typically a group of 2, were heated under vacuum at approximately 150

°C to drive off superficially trapped atmospheric Ar. Each individual sample was heated in 4 steps at 250, 375, 500 and 1000 °C. For the first 3 steps, the heating period was about 24 h, but the heating at 1000 °C was only for 20 min. The temperatures used in this study were chosen on the basis of preliminary experiments and on information from the literature (Odin and Bonhomme 1982; Zimmermann and Odin 1982; Sedivy et al. 1984) concerning the release of Ar from these types of clay during stepwise heating. The heating intervals were selected on the basis of preliminary experiments showing that after 24 h of heating at a given temperature, the rate of Ar release is very small. Preliminary experiments also showed that at 1000 °C not more than 20 min is needed for all of the remaining Ar to come out of clay-sized particles. The Ar released during each step was spiked with  $^{38}\text{Ar}$  and analyzed by mass spectrometry, so that the amount of radiogenic Ar released in each step could be calculated. Blank runs were used to show that the amount of Ar coming from equipment was small and could be accounted for by an atmospheric-Ar correction based upon the measured amount of  $^{36}\text{Ar}$ .

The kinetics of Ar release from several of the samples was examined in greater detail in experiments in which Ar was removed and measured at a number of intervals during 24 h, but sometimes longer, of heating at constant temperature. Such Ar samples were not spiked with  $^{38}\text{Ar}$ , but were transferred to the mass spectrometer in such a way that the signal from the mass spectrometer would be in fixed proportion to the amount of Ar. Note that the sensitivity of the MS-10 mass spectrometer is quite stable over time. Runs with spikes were done frequently enough to establish that the uncertainty in the amount of Ar in an unspiked run should not exceed 5%.

After the Ar analyses of a sample were completed, the K and Fe of the same sample were measured by flame atomic absorption spectrophotometry of material released by dissolving the capsule and its contents in hydrofluoric acid. The K content of the fused quartz is only about 1 ppm, so the contribution of K from the glass (<1  $\mu\text{g}$ ) is negligible.

## RESULTS

The K and Fe contents and the radiogenic Ar released by stepwise heating of the sized clay samples are shown in Table 2. The illite samples have high K contents but low Fe contents, and the glauconitic samples have high Fe contents and medium to high K contents (Figure 1). The variability in composition among different size fractions of each sample is generally less than the variability among the different samples of each kind. Only the glauconitic sample TWG shows notable variability in K and Fe content among the different fractions.

Table 2. Potassium and Fe contents and radiogenic Ar ( $^{40}\text{Ar}_{\text{rad}}$ ) released by stepwise heating of illitic and glauconitic clay samples.

Sample	Size range ( $\mu\text{m}$ )	Sample mass (mg)	K (%)	Fe (%)	Temperature ( $^{\circ}\text{C}$ )	$^{40}\text{Ar}_{\text{rad}}$ (%)	$^{40}\text{Ar}_{\text{rad}}$ (ng/g)	Sum $^{40}\text{Ar}_{\text{rad}}$ (%)
EI	2–0.5	20.0	6.82	1.39	250	26.1	0.12	0.1
					375	89.9	8.1	6.4
					500	96.2	65.9	51.8
					1000	94.0	53.0	41.7
	<0.5	20.0	6.78	1.27	250	26.1	0.1	0.1
					375	91.7	11.9	9.4
					500	96.0	61.6	48.8
					1000	90.8	52.7	41.7
HI	0.5–0.2	40.1	7.36	2.79	250	9.9	0.16	0.5
					375	37.4	1.29	4.0
					500	61.8	4.45	13.7
					1000	80.8	26.6	81.8
	<0.2	40.3	7.18	2.34	250	7.5	0.14	0.9
					375	23.5	0.49	3.0
					500	19.8	0.98	5.9
					1000	83.0	14.81	90.2
G294	2–0.5	20.0	5.68	10.0	250	70.8	1.97	1.3
					375	96.7	74.4	49.4
					500	96.4	73.6	48.7
					1000	41.8	1.06	0.7
	0.5–0.2	20.0	5.49	10.1	250	68.9	2.29	1.7
					375	97.4	65.4	49.7
					500	97.6	62.9	47.8
					1000	36.9	1.06	0.8
	<0.2	20.0	5.88	10.3	250	66.4	1.01	0.7
					375	96.5	71.5	47.6
					500	96.6	77.2	51.4
					1000	27.0	0.5	0.3
G1392	0.5–0.2	10.0	3.81	13.6	250	30.0	0.36	0.9
					375	88.7	31.8	78.5
					500	66.4	7.60	18.8
					1000	13.5	0.75	1.8
TWG	<2	86.4	3.36	16.7	250	22.7	0.72	8.3
					375	36.6	6.72	77.3
					500	59.9	1.14	13.1
					1000	16.5	0.12	1.3
	2–0.5	100.0	2.88		250	21.2	0.11	1.7
					375	47.1	5.13	80.2
					500	67.9	1.09	17.1
					1000	11.0	0.06	1.0
	0.5–0.2†	16.5	3.23	13.4	250		0.63	10.7
					375		3.82	67.9
					500		0.65	11.6
					1000		0.57	9.8
	0.2–0.1	97.9	2.90		250	18.4	0.10	1.6
					375	54.9	5.03	81.2
					500	51.0	1.07	17.2
					1000	0.1	0.00	0.0
	<0.1‡	15.4	4.12	17.0	250		0.84	10.3
					375		5.85	68.0
					500		1.34	16.7
					1000		0.42	5.0
Pellets§	20.0	5.29	17.2	250	28.5	0.19	1.8	
				375	48.6	7.85	76.3	
				500	53.5	2.01	19.5	
				1000	24.5	0.25	2.4	

† Average of 2 runs.

‡ Average of 3 runs.

§ Hand-picked pellets, more fully evolved than the typical pellets of the glauconitic rock from which the TWG size fractions were separated.

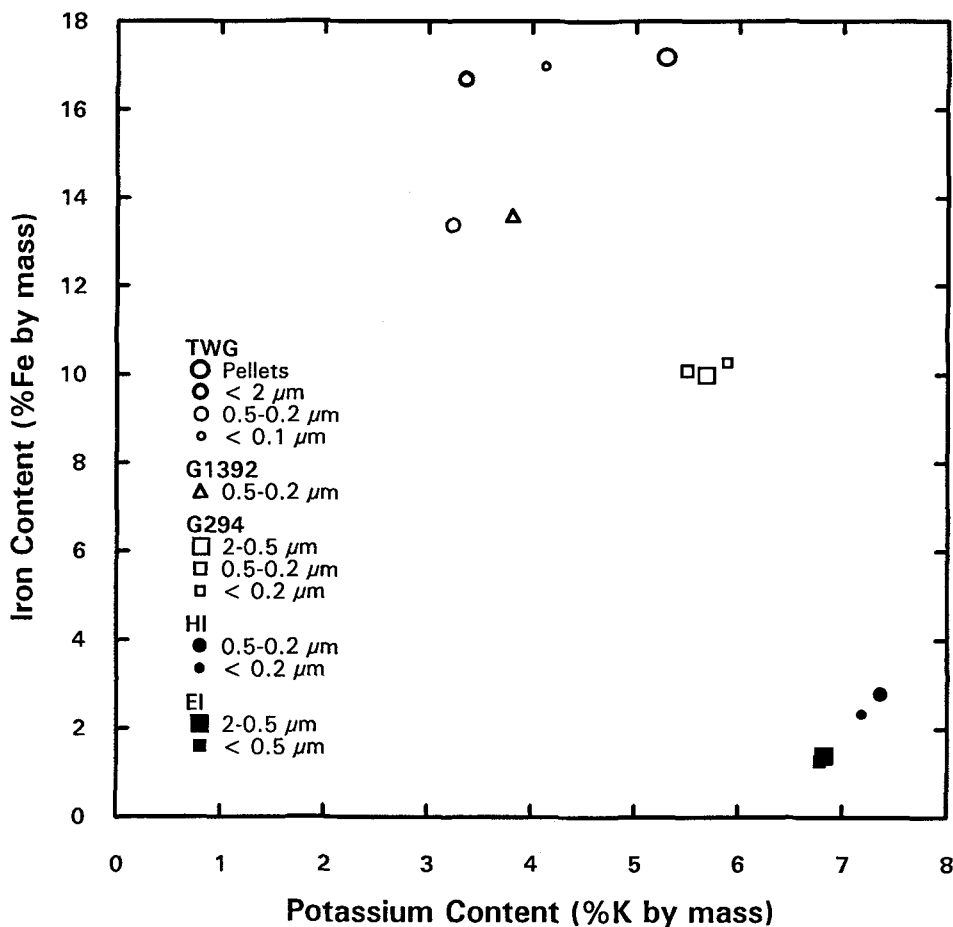


Figure 1. Iron content versus K content for various size fractions of glauconite or glauconite/smectite (open symbols) and illite (closed symbols) samples. Different particle sizes are indicated schematically by the different sizes of the symbols.

The results of the stepwise-heating experiments are presented in Table 2 and are shown in Figure 2 as plots of the cumulative fraction of radiogenic Ar released from each size fraction as a function of the heating temperature. The yields of radiogenic Ar from the glauconitic samples are distinctly different functions of temperature than those from illite. After 24 h at 375 °C, each illite sample had released only a small fraction of its radiogenic Ar, but the glauconitic samples had released one-half or more of their radiogenic Ar. After 24 h at 500 °C, the glauconitic samples had released nearly all of their radiogenic Ar but the illites had released not more than 60% of theirs.

There is very little difference in the results of the stepwise-heating experiments among the different size fractions of any sample. The greatest variability is among the various size fractions of TWG, which are also the most variable in Fe and K content. There is no indication of relatively more rapid loss of radiogenic Ar from the finer size fractions than from the coarser fractions.

Additional samples of some of the sized clays and hand-picked glauconitic pellets were analyzed for the purpose of obtaining more-detailed information on the kinetics of radiogenic Ar release from these materials at the same temperatures used in the earlier experiments. The results of these experiments are listed in Table 3 and are depicted in Figure 3 as the cumulative fraction of the radiogenic Ar in each sample released as a function of the time of heating at each of several temperatures.

## DISCUSSION

### Argon Yields in Relation to Particle Size

For each of the size-fractionated samples, the fraction of radiogenic Ar released at each temperature in the heating schedule is about the same for all size fractions of the sample (Table 2). That the Ar yields do not depend upon particle size was unexpected, because the dependence of radiogenic Ar yield upon particle size during stepwise heating under vacuum has been demonstrated for book mica (Evernden et al. 1960) and for

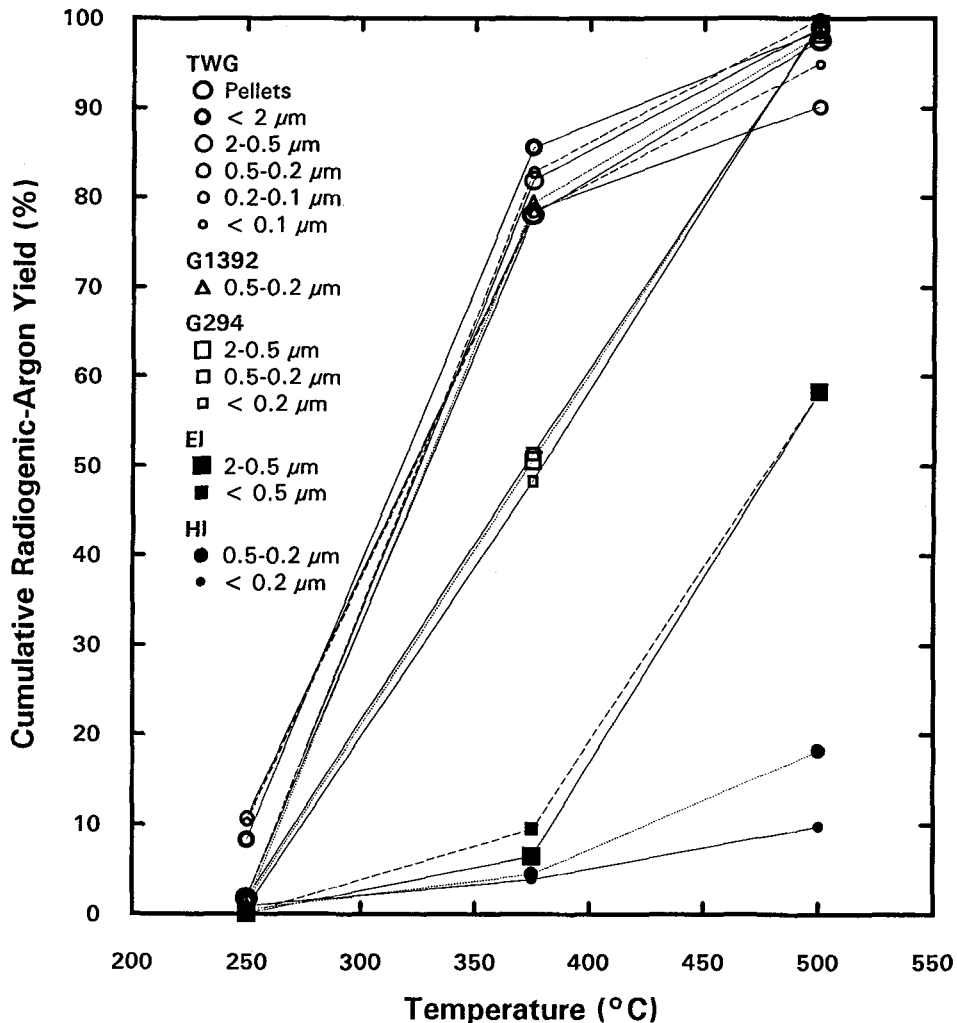


Figure 2. Cumulative yields of radiogenic Ar for the 24-h heating steps. Yields for each sample are relative to the total amount of radiogenic argon measured for that sample (Table 2, last column). The symbols are the same as those used in Figure 1. For clarity where points are overlapping, the 3 points for each sample are connected to one another by straight line segments.

white mica (illite) from very low grade (anchizonal) slates and metatuffs (Reuter and Dallmeyer 1987a, 1987b). It has long been recognized that the release of Ar from micas during heating under vacuum is related to structural changes associated with dehydroxylation, but the kinetics of dehydroxylation may be controlled by diffusion of  $\text{H}_2\text{O}$  molecules from the dehydroxylating material (Evernden et al. 1960; Stoch 1984) and thus be dependent upon particle size. Stoch (1991) interpreted differential thermal analyses of phyllosilicates, including low-defect clay minerals, to indicate that the energy required for dehydroxylation increases as crystal size increases because of a diffusion barrier to  $\text{H}_2\text{O}$  loss. He suggested, however, that when grains are very small ( $<1 \mu\text{m}$ ), or are strongly defect, no diffusion barrier exists to keep the gas inside.

One way to explain the absence of a particle-size effect on the Ar yields in this study is to suppose that the effective particle size for loss of water vapor by diffusion and for concomitant Ar loss is in all size fractions equal to or less than the size of the smallest particles. For example, even in well-evolved glauconite there is evidence that particles consist of very small crystallites—packets of 10 or so mica-type layers whose largest dimension is typically not greater than  $0.1 \mu\text{m}$  (Amouric and Parron 1985). Similar packet sizes have been observed in illites of low crystallinity, although higher-grade illites have considerably larger crystallites (Merriman et al. 1990; Dong et al. 1995). The samples used in this study were not examined by techniques that would show structural details at the sub-micrometer level, so the

Table 3. Argon yields obtained in detailed kinetic studies.

Sample	Temperature (°C)	Cumulative heating time (h)	Cumulative radiogenic-Ar yield (%)	
TWG <2 μm	250	1	2.6	
		6	4.5	
		12	5.1	
		24	8.4	
	375	25	43.4	
		33	65.2	
		48	81.1	
		57	96.5	
	500	57	98.2	
		72	98.4	
	1000	72.3	100.0	
	TWG pellets	250	1	1.6
4			3.8	
7			4.5	
12			4.3	
375		24	6.9	
		25	44.5	
		28	57.2	
		30	60.7	
		36	66.7	
		48	72.6	
500		49	94.1	
		52	95.7	
		54	95.3	
		60	95.8	
		72	96.7	
		1000	48	100.0
Bashi pellets		250	1	0.9
			3.5	0.9
	7		1.2	
	12		1.3	
	375	24	1.7	
		24.5	16.0	
		28	25.6	
		30	29.9	
		36	34.9	
		48	42.1	
	500	49	63.7	
		52	80.2	
		54	83.7	
		60	88.4	
		72	92.2	
		1000	72.3	100.0
	HI <2 μm	250	1	0.3
			6	0.4
24			0.4	
375		25	1.1	
		33	2.8	
		48	3.6	
500		49	5.2	
		57	12.4	
		72	18.4	
1000		72.3	100.0	
HI <0.2 μm		250	24	0.8
			25	1.5
	30		2.7	
	375	36	2.5	
		48	2.7	
		49	3.8	
	500	54	6.1	
		65	6.7	
		72	6.9	
	1000	72.3	100.0	

possibility that there was no appreciable difference in effective particle size among the various size fractions cannot be further evaluated.

An alternative explanation of the absence of a particle-size effect on Ar yields for these clay-sized materials can be based on the suggestion of Stoch (1991) that for such fine materials the kinetics of dehydroxylation is controlled by the rate of chemical dissociation because there is no diffusion barrier for the escaping H<sub>2</sub>O. This idea is consistent with the observations of Brindley and Nakahira (1957), who used thermogravimetric measurements to infer a first-order mechanism for dehydroxylation of fine-grained kaolinite and halloysite. Suitch (1986) has presented direct evidence in support of the mechanism proposed by Brindley and Nakahira that "either crystallites are fully reacted to form metakaolinite or they remain unreacted and structurally identical with their unheated predecessor". No such definitive work on the dehydroxylation of glauconite and illite has been done, but if Stoch's idea that there is no diffusion barrier to the loss of hydroxyl H<sub>2</sub>O from clay-sized material is applicable to these clays as well as to fine kaolinite, then a particle-size effect on Ar release should not be expected provided that dehydroxylation frees the Ar.

#### Relation of Ar Yields to Composition

Among the glauconitic samples, Ar was released more readily from the samples having lower K content (Figures 2 and 3). Although no chemical analysis of the Bashi pellets was done as part of this study, a K content of 6.6% for Bashi pellets from Clay County, Georgia, was obtained by Wampler (1973). It has been well-established that the degree of ordering of glauconite/smectite increases as the K content increases (Burst 1958; Hower 1961; Thompson and Hower 1975; Odin and Dodson 1982), and it is reasonable to expect that the degree of ordering influences the activation energy for dehydroxylation.

The Ar yields at lower temperature are much less for the illite samples than for the glauconitic samples (Figure 2). These illite samples have more K than any of the glauconitic samples, which implies a higher degree of crystallinity for the illites. In addition to having lower K contents, the glauconitic samples are much richer in Fe than the illites. Dehydroxylation occurs at lower temperature among Fe-rich smectites than among smectites having little Fe, because the Fe-hydroxyl bond is weaker than the aluminum-hydroxyl bond (Killingsley and Day 1990; Levy 1990), so the lower temperature Ar release from the glauconitic samples can be attributed in part to their higher Fe contents than the illites. Figure 4 is a plot of the sum of the radiogenic Ar yields from the first 2 heating steps, at 250 and 375 °C, against the atomic ratio of Fe to K. The general trend of the plotted data is con-

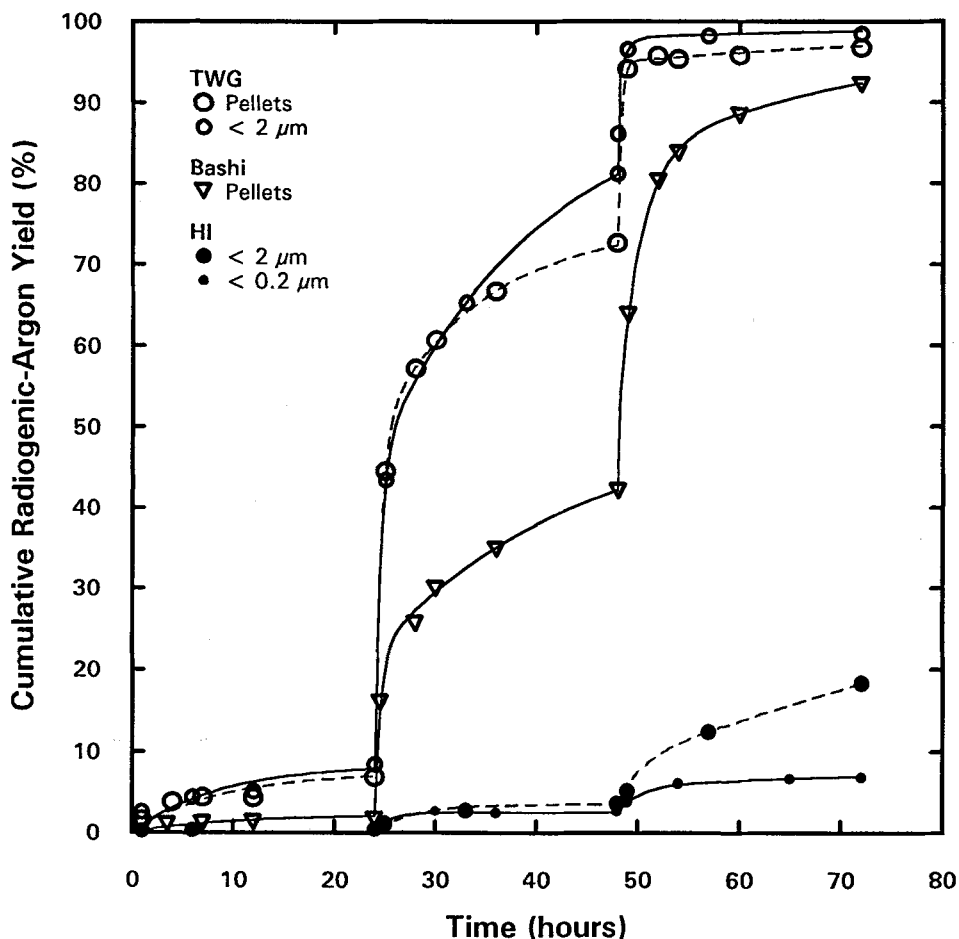


Figure 3. Results of experiments on the kinetics of Ar release during the 24-h heating steps. The cumulative yield of radiogenic Ar is shown as a function of time for 3 heating steps of 24 h each at 250, 375 and 500 °C (Table 3). The curved lines that approximately match the data sets were generated by simulation of reactions that follow first-order kinetics.

sistent with the idea that Ar is released more easily as K content decreases and/or as Fe content increases.

#### Kinetic Models

Experimental measurements of dehydroxylation of various clays have been fitted to diffusion models and to first- and second-order reaction models in attempts to ascertain what controls the rate of dehydroxylation, but these efforts have not led to a consensus on an appropriate model (Killingsley and Day 1990). Zimmermann and Odin (1982) measured both the radiogenic Ar and the H<sub>2</sub>O released by stepwise heating of 5 glauconitic samples that were not size fractionated. They then modeled the results as volume diffusion from equisized spherical particles to find a single value, for each sample, for activation energy for diffusion of each of the 2 volatile substances (H<sub>2</sub>O and Ar). They recognized, however, that such modeling "is greatly dependent on physical assumptions which may not be wholly appropriate because of the diversity of

natural materials and phenomena". From their diffusion model they found activation energies for release of Ar from 70 to 120 kJ mol<sup>-1</sup>, generally increasing with increasing K content, and somewhat lower activation energies for release of hydroxyl H<sub>2</sub>O. They also measured the H<sub>2</sub>O released from samples under linearly increasing temperature and fit the data to a first-order reaction model, finding activation energies for H<sub>2</sub>O release about the same as those obtained from the diffusion model applied to the stepwise-heating data. Bray et al. (1987) used data on Ar released by stepwise heating to infer an activation energy of 150 kJ mol<sup>-1</sup> for Ar diffusion from a sample of illite from the Athabasca Basin.

It must be pointed out that if a diffusion model for equisized particles of homogeneous material is applied to data from material having a range of effective diffusion distances or a range of activation energies for diffusion, or both (that is, having a range for the effective value of the diffusion parameter  $D/a^2$ ), then the

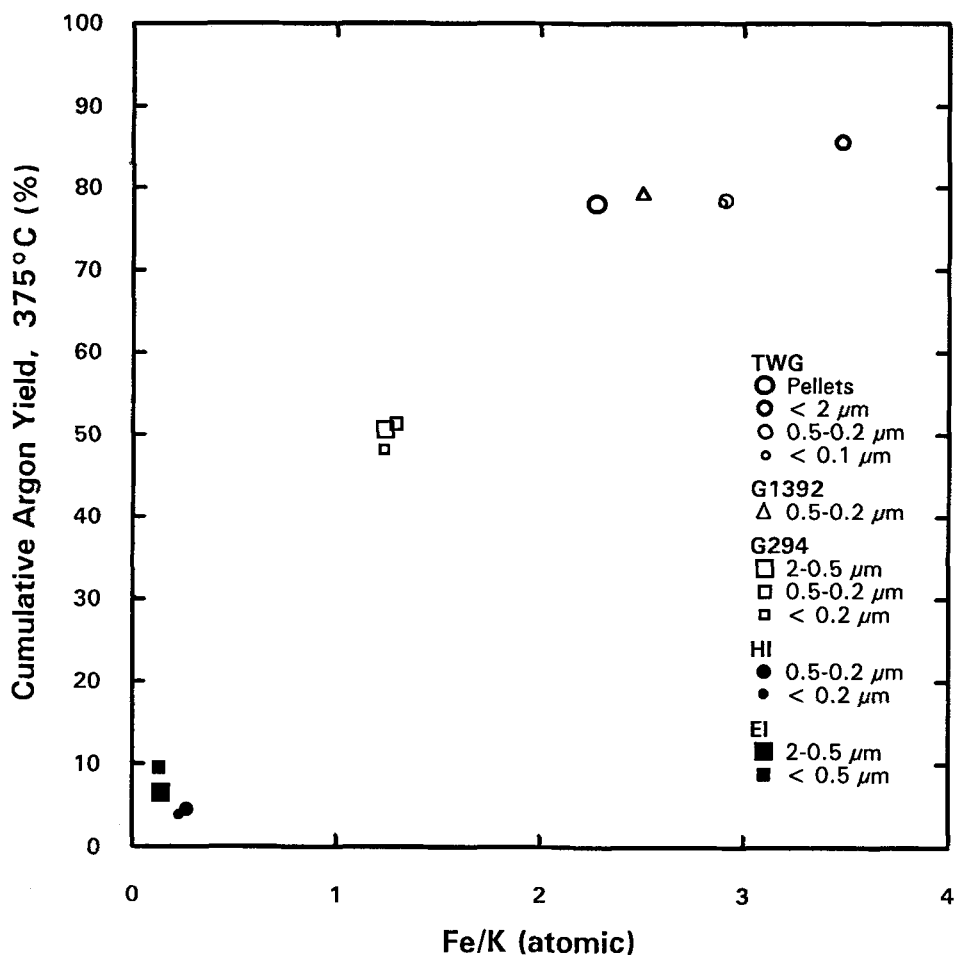


Figure 4. Cumulative yield of radiogenic Ar for the first 2 heating steps (at 250 and 375 °C) against the ratio of amount of Fe to amount of K.

activation energy calculated from an Arrhenius plot will not be physically meaningful (McDougall and Harrison 1988, Chapter 5). Specifically, the more complete release at lower temperatures of volatiles from portions of the sample for which the effective diffusion parameter is relatively large would bias an Arrhenius plot so that the inferred activation energy would be too low. For similar reasons, if data from a material that decomposes with first-order kinetics but is heterogeneous in respect to the activation energy for decomposition are fit to a model with a single value for activation energy, one may expect that the activation energy calculated from decomposition rates at different temperatures will be deceptively low.

It has been well-established that glauconitic material is often mineralogically heterogeneous. Within the grains of such material, the green clay may be in different stages of evolution (Odin and Fullagar 1988). On a finer scale, ordering in glauconite/smectite and illite/smectite extends only nanometers in a direction

perpendicular to the layers (Amouric and Parron 1985; Środoń et al. 1990; Veblen et al. 1990). Furthermore, diagenetic illite appears to be compositionally heterogeneous on a nanometer scale even after expandability has been reduced to near zero by K uptake (Aronson and Douthitt 1986; Środoń et al. 1986), and the same may be true of glauconite crystallites in well-evolved glauconitic material. It would be futile to attempt to determine the nature of the process of Ar loss and related dehydroxylation for such material by fitting experimental data to models that are too simple to represent the material adequately.

Because there is reason to believe that dehydroxylation of clays follows first-order kinetics, it should be instructive to simulate the observed kinetics of Ar release as a first-order process. The results of such simulations are presented as curves that approximately match the data points of Figure 3. The curves were obtained by trial and error from the presumption that each sample consists of one or more components, each



having a discrete activation energy for loss of its radiogenic Ar via a first-order process (dehydroxylation). A rather arbitrary assumption that the activation energies should be of the order of  $200 \text{ kJ mol}^{-1}$  led to the use of  $1 \times 10^{12} \text{ s}^{-1}$  as the pre-exponential factor in the Arrhenius equation for the first-order rate constants used in the simulations. The value  $200 \text{ kJ mol}^{-1}$ , which is  $47.8 \text{ kcal mol}^{-1}$ , is several times greater than the values of activation energy found by Thompson and Hower (1973) for release of K from glauconite by acid dissolution. The structural breakdown needed for dehydroxylation and Ar loss is envisioned as requiring more energy than does loss of interlayer K to an acid solution. The value  $200 \text{ kJ mol}^{-1}$  is also greater than the activation energies inferred by Zimmerman and Odin (1982) for Ar loss from glauconitic samples and by Bray et al. (1987) for Ar loss from illite, but those inferences appear to be based on inadequate models.

None of the data sets can be simulated adequately with a single value for the activation energy. For each glauconitic sample, at least 4 different values of activation energy are needed to simulate the data reasonably well, and 5 values were used to produce the closely fitting curves shown in Figure 3. The parameters used to generate these curves are listed in Table 4. The activation energies for the hypothetical components of the 3 glauconitic samples are closely similar in all cases except Component 4. Possibly glauconitic clay has distinct components having discrete activation energies that differ from one another because of discrete differences in layer charge or because of differences in the ordering of layers as reflected in the Reichweite ordering parameter. Conversely, it is possible that the prevalence of certain values of activation energy is somehow an artifact of the particular heating schedule used in the experiments. In reality the activation energies in glauconitic clay may vary continuously, with a distribution that is shifted toward higher energy in the case of the Bashi pellets, which are richer in K than the TWG samples.

Since the illite samples released only small fractions of their radiogenic Ar during the part of the heating schedule in which detailed kinetic information was obtained, there is little to be inferred about the nature of the illite from these experiments. It is obvious that if the Ar loss from illite follows first-order kinetics, virtually all of the Ar in the HI samples is in particles having a higher activation energy for Ar release than do the particles in glauconite.

These simulations suggest that if Ar is released from glauconitic clay during heating under vacuum according to first-order kinetics, then there are different Ar-bearing materials in the clay for which different energies are needed to activate the Ar release. Since typical glauconitic materials are known to be structurally and chemically heterogeneous, it would be reasonable to continue to investigate the hypothesis that Ar release from glauconitic clay (and from illite) during

Table 4. Values of parameters used to simulate observed Ar-release kinetics.

Hypothetical component	TWG <2 $\mu\text{m}$	TWG pellets	Bashi pellets	HI <2 $\mu\text{m}$	HI <0.2 $\mu\text{m}$
Relative amount of radiogenic Ar (%)					
Component 1	8	7	2	3.5	2.5
Component 2	38	42	20	5.5	3.5
Component 3	45	23	28	91	94
Component 4	7	23	33		
Component 5	2	5	17		
Activation energy ( $\text{kJ mol}^{-1}$ )†					
Component 1	165	165	165	200	195
Component 2	190	190	190	236	236
Component 3	208	205	209	265	280
Component 4	228	223	235		
Component 5	255	255	252		

† The activation energies are based on an arbitrary choice of  $1 \times 10^{12} \text{ s}^{-1}$  as the pre-exponential factor in the Arrhenius equation, so the values of the activation energies listed here have significance only relative to one another.

heating under vacuum is the result of a dissociation reaction that follows first-order kinetics.

## CONCLUSIONS

The conclusions of the present study may be stated as follows:

1) The cumulative yield of radiogenic Ar at each temperature in the heating schedule is about the same for all size fractions of each sample analyzed, indicating that Ar yields from these materials do not depend upon particle size.

2) Ar is released more readily from low-K, high-Fe glauconitic samples than from those having more K and/or less Fe, which demonstrates a significant influence of the chemistry of the minerals on the Ar release process.

3) Under an assumption of first-order kinetics, more than 2 values of activation energy are required to simulate the observed release of Ar from glauconitic samples, which is consistent with the known heterogeneity of such material.

Since Ar yields from glauconitic and illitic clay samples seem to be independent of particle size, the hypothesis that Ar release from such materials follows first-order kinetics should be investigated further. More-detailed studies of the kinetics of Ar release from carefully characterized glauconitic and illitic samples should provide information useful to those who will be using K-Ar relationships to shed light on the processes of diagenesis and particularly to those who will be attempting to use the  $^{40}\text{Ar}/^{39}\text{Ar}$  method for study of K-Ar relationships in such materials.

## ACKNOWLEDGMENTS

The authors thank E. Eslinger and G. Thompson for providing samples used in this study. S. Pickering pointed out the glauconitic sand in the Twiggs Clay. Comments by E.

Eslinger, R. C. Walker and an anonymous reviewer on an earlier manuscript that included the work presented here were of considerable value in the preparation of this paper. The authors thank E. Eslinger and N. Clauer for thoughtful reviews of this paper.

## REFERENCES

- Amouric M, Parron C. 1985. Structure and growth mechanism of glauconite as seen by high-resolution transmission electron microscopy. *Clays Clay Miner* 33:473–482.
- Aronson JL, Douthitt CB. 1986. K/Ar systematics of an acid-treated illite/smectite: Implications for evaluating age and crystal structure. *Clays Clay Miner* 34:473–482.
- Aronson JL, Hower J. 1976. Mechanism of burial metamorphism of argillaceous sediment: 2. Radiogenic argon evidence. *Geol Soc Am Bull* 87:738–744.
- Bray CJ, Spooner ETC, Hall CM, York D, Bills TM, Krueger HW. 1987. Laser probe  $^{40}\text{Ar}/^{39}\text{Ar}$  and conventional K/Ar dating of illites associated with the McClean unconformity-related uranium deposits, north Saskatchewan, Canada. *Can J Earth Sci* 24:10–23.
- Brindley GW, Nakahira M. 1957. Kinetics of dehydroxylation of kaolinite and halloysite. *J Am Ceram Soc* 40:346–350.
- Burst, JF. 1958. Mineral heterogeneity in “glauconite” pellets. *Am Mineral* 43:481–497.
- Dong H, Hall CM, Peacor DR, Halliday AN. 1995. Mechanisms of argon retention in clays revealed by laser  $^{40}\text{Ar}$ - $^{39}\text{Ar}$  dating. *Science* 267:355–359.
- Evernden JF, Curtis GH, Kistler RW, Obradovich J. 1960. Argon diffusion in glauconite, microcline, sanidine, leucite, and phlogopite. *Am J Sci* 258:583–604.
- Evernden JF, Curtis GH, Obradovich J, Kistler R. 1961. On the evaluation of glauconite and illite for dating sedimentary rocks by the potassium-argon method. *Geochim Cosmochim Acta* 23:78–99.
- Hower J. 1961. Some factors concerning the nature and origin of glauconite. *Am Mineral* 46:313–334.
- Hurley PM. 1966. K-Ar dating of sediments. In: Schaeffer OA, Zähringer J, compilers. *Potassium argon dating*. New York: Springer-Verlag. p 134–151.
- Killingsley JS, Day SJ. 1990. Dehydroxylation kinetics of kaolinite and montmorillonite from Queensland Tertiary oil shale deposits. *Fuel* 69:1145–1149.
- Levy JH. 1990. Effect of water vapor pressure on the dehydroxylation and dehydroxylation of kaolinite and smectite isolated from Australian Tertiary oil shales. *Energy Fuels* 4:146–151.
- Liewig N, Mossmann J-R, Clauer N. 1987. Datation isotopique K-Ar d'argiles diagénétiques de réservoirs gréseux: mise en évidence d'anomalies thermiques du Lias inférieur en Europe nord-occidentale. *CR Acad Sci Ser II* 304:707–711.
- McDougall I, Harrison TM. 1988. *Geochronology and thermochronology by the  $^{40}\text{Ar}/^{39}\text{Ar}$  Method*. New York: Oxford Univ Pr. 212 p.
- Merriman RJ, Roberts B, Peacor DR. 1990. A transmission electron microscope study of white mica crystallite size distribution in a mudstone to slate transitional sequence, North Wales, UK. *Contrib Mineral Petrol* 106:27–40.
- Odin GS, Bonhomme MG. 1982. Argon behaviour in clays and glauconies during preheating experiments. In: Odin GS, editor. *Numerical dating in stratigraphy*. Chichester, UK: J Wiley. p 333–343.
- Odin GS, Dodson MH. 1982. Zero isotopic age of glauconies. In: Odin GS, editor. *Numerical dating in stratigraphy*. Chichester, UK: J Wiley. p 277–305.
- Odin GS, Fullagar PD. 1988. Geological significance of the glaucony facies. In: Odin GS, editor. *Green marine clays: oolitic ironstone facies, verdine facies, glaucony facies and celadonite-bearing facies—a comparative study*. Amsterdam: Elsevier Science. p 295–332.
- Polevaya NI, Murina GA, Kazakov GA. 1961. Utilization of glauconite in absolute dating. *Ann NY Acad Sci* 91:298–310.
- Reuter A, Dallmeyer RD. 1987a. Significance of  $^{40}\text{Ar}/^{39}\text{Ar}$  age spectra of whole-rock and constituent grain-size fractions from anchizonal slates. *Chem Geol (Isot Geosci)* 66:73–88.
- Reuter A, Dallmeyer RD. 1987b.  $^{40}\text{Ar}/^{39}\text{Ar}$  dating of cleavage formation in tuffs during anchizonal metamorphism. *Contrib Mineral Petrol* 97:352–360.
- Sardarov SS. 1961. Bond energy and retention of radiogenic argon in micas. *Geochemistry for 1961*. p 33–44 (Translated from *Geokhimiya* 1961. p 30–38).
- Sardarov SS. 1963. Preservation of radiogenic argon in glauconites. *Geochemistry for 1963*. p 937–944 (Translated from *Geokhimiya* 1963. p 905–911).
- Sedivy RA, Wampler JM, Weaver CE. 1984. Potassium-argon. In: Weaver CE and Associates. *Shale-slate metamorphism in southern Appalachians*. Amsterdam: Elsevier Science. p 153–183.
- Smith PE, Evensen NM, York D. 1993. First successful  $^{40}\text{Ar}/^{39}\text{Ar}$  dating of glauconies: Argon recoil in single grains of cryptocrystalline material. *Geology* 21:41–45.
- Śródoń J, Andreoli C, Elsass F, Robert M. 1990. Direct high-resolution transmission electron microscopic measurement of expandability of mixed-layer illite/smectite in bentonite rock. *Clays Clay Miner* 38:373–379.
- Śródoń J, Morgan DJ, Eslinger EV, Eberl DD, Karlinger MR. 1986. Chemistry of illite/smectite and end-member illite. *Clays Clay Miner* 34:368–378.
- Stoch L. 1984. Significance of structural factors in dehydroxylation of kaolinite polytypes. *J Therm Anal* 29:919–931.
- Stoch L. 1991. Explosive thermal dehydration of solids. *J Therm Anal* 37:1415–1429.
- Suitch PR. 1986. Mechanism for the dehydroxylation of kaolinite, dickite, and nacrite from room temperature to 455 °C. *J Am Ceram Soc* 69:61–65.
- Thompson JR, Hower J. 1973. An explanation for low radiometric ages from glauconite. *Geochim Cosmochim Acta* 37:1473–1491.
- Thompson JR, Hower J. 1975. The mineralogy of glauconite. *Clays Clay Miner* 23:289–300.
- Veblen DR, Guthrie GD, Jr, Livi KJT, Reynolds RR, Jr. 1990. High-resolution transmission electron microscopy and electron diffraction of mixed-layer illite/smectite: Experimental results. *Clays Clay Miner* 38:1–13.
- Wampler JM. 1973. Age dating of rocks to assist in understanding the geological history of Georgia Piedmont area. Atlanta: Georgia Institute of Technology. Unpublished technical report for Project No. G-35-602.
- Wampler JM, Thoroman MC, Padan A. 1985. A microanalytical technique for potassium-argon analysis of clay. *Geol Soc Am Abstr Programs* 17:411.
- Weaver CE, Wampler JM. 1970. K, Ar, illite burial. *Geol Soc Am Bull* 81:3423–3430.
- Zimmermann J-L, Odin GS. 1977. Cinétique de la libération de l'argon de l'eau et des composés carbonés dans le matériel de référence glauconite GL-O. *Bull Minéral* 102:48–55.
- Zimmermann J-L, Odin GS. 1982. Kinetics of the release of argon and fluids from glauconies. In: Odin GS, editor. *Numerical dating in stratigraphy*. Chichester, UK: J Wiley. p 345–362.

(Received 8 February 1995; accepted 27 December 1995; Ms. 2619)